


















Galaxy And Mass Assembly: Galaxy Morphology in the Green Valley, Prominent rings and looser Spiral Arms

Dominic Smith¹ , Lutz Habertzettl¹ , L. E. Porter¹ , Ren Porter-Temple¹ ,
 Christopher P. A. Henry¹ , Benne Holwerda¹ *, Á. R. López-Sánchez^{2,3,4} ,
 Steven Phillipps⁵ , Alister W. Graham⁶ , Sarah Brough⁷ , Kevin A. Pimbblet⁸ ,
 Jochen Liske¹⁰ , Lee S. Kelvin¹¹ , Clayton D. Robertson¹ , Wade Roemer¹,
 Michael Walmsley¹² , David O’Ryan¹³  and Tobias Géron¹³ .

¹ *Department of Physics and Astronomy, University of Louisville*

² *Australian Astronomical Optics, Macquarie University, 105 Delhi Rd, North Ryde, NSW 2113, Australia*

³ *Department of Physics and Astronomy, Macquarie University, NSW 2109, Australia*

⁴ *ARC Centre of Excellence for All Sky Astrophysics in 3 Dimensions (ASTRO-3D)*

⁵ *Astrophysics Group, School of Physics, University of Bristol, Tyndall Avenue, Bristol BS8 1TL, UK*

⁶ *Centre for Astrophysics and Supercomputing, Swinburne University of Technology, Hawthorn, VIC 3122, Australia*

⁷ *School of Physics, University of New South Wales, NSW 2052, Australia*

⁸ *E.A.Milne Centre for Astrophysics, University of Hull, Cottingham Road, Kingston-upon-Hull, HU6 7RX, UK*

¹⁰ *Hamburger Sternwarte, Universität Hamburg, Gojenbergsweg 112, 21029 Hamburg, Germany*

¹¹ *Department of Astrophysical Sciences, Princeton University, 4 Ivy Lane, Princeton, NJ 08544, USA*

¹² *Jodrell Bank Centre for Astrophysics, Department of Physics & Astronomy, University of Manchester, Oxford Road, Manchester M13 9PL, UK*

¹³ *Observational Astrophysics Group, Lancaster University, LA1 4YW, UK*

¹⁴ *Department of Physics, University of Oxford, Denys Wilkinson Building, Keble Road, Oxford OX1 3RH, UK*

Accepted XXX. Received YYY; in original form ZZZ

ABSTRACT

Galaxies broadly fall into two categories: star-forming (blue) galaxies and quiescent (red) galaxies. In between, one finds the less populated “green valley”. Some of these galaxies are suspected to be in the process of ceasing their star-formation through a gradual exhaustion of gas supply or already dead and are experiencing a rejuvenation of star-formation through fuel injection. We use the Galaxy And Mass Assembly database and the Galaxy Zoo citizen science morphological estimates to compare the morphology of galaxies in the green valley against those in the red sequence and blue cloud. Our goal is to examine the structural differences within galaxies that fall in the green valley, and what brings them there. Previous results found disc features such as rings and lenses are more prominently represented in the green valley population. We revisit this with a similar sized data set of galaxies with morphology labels provided by the Galaxy Zoo for the GAMA fields based on new KiDS images. Our aim is to compare qualitatively the results from expert classification to that of citizen science.

We observe that ring structures are indeed found more commonly in green valley galaxies compared to their red and blue counterparts. We suggest that ring structures are a consequence of disc galaxies in the green valley actively exhibiting characteristics of fading discs and evolving disc morphology of galaxies. We note that the progression from blue to red correlates with loosening spiral arm structure.

Key words: galaxies: bar, galaxies: bulges, galaxies: disc, galaxies: evolution, galaxies: spiral, galaxies: star formation

1 INTRODUCTION

Previous large-scale surveys of galaxies have revealed a bi-modality in the colour-magnitude diagram of galaxies with two distinct populations: one with blue optical colours and another with red optical colours (Strateva et al. 2001; Baldry et al. 2004; Bell et al. 2004; Martin et al. 2007; Faber et al. 2007; Baldry et al. 2006; Willmer et al. 2006; Ball et al. 2008; Brammer et al. 2009; Mendez et al.

2011; Taylor et al. 2015; Corcho-Caballero et al. 2020, 2021). These populations were dubbed the “blue cloud” (BC), or “star-forming galaxy sequence”, and the “red sequence” (RS) respectively (Driver et al. 2006; Faber et al. 2007; Salim 2015). The blue cloud and red sequence are best separated at higher stellar mass and mix at lower stellar masses (cf. Taylor et al. 2015).

The Galaxy Zoo (GZ) project (Lintott et al. 2008), which produced morphological classifications for a million galaxies, helped to confirm that this bi-modality is not entirely morphology driven (Salim et al. 2007; Schawinski et al. 2007; Bamford et al. 2009; Skibba et al.

* Corresponding author, E-mail: benne.holwerda@louisville.edu

2009, Figure 1). It suggested larger fractions of spiral galaxies in the red sequence¹ (Masters et al. 2010) and elliptical galaxies in the blue cloud (Schawinski 2009) than had previously been detected.

The sparsely populated colour-mass space between these two populations, the so-called “Green Valley” (green valley) (Figure 2), provides clues to the nature and duration of a galaxies’ transitions from blue cloud to red sequence. This transition must occur on rapid timescales, otherwise there would be an accumulation of galaxies residing in the green valley, rather than an accumulation in the red sequence as is observed (Arnouts et al. 2007; Martin et al. 2007; Smethurst et al. 2015, 2017; Nogueira-Cavalcante et al. 2017; Bremer et al. 2018; Phillipps et al. 2019; Barone et al. 2022). Alternatively, gas infall onto red sequence galaxies may rejuvenate them into the green valley (e.g. Graham et al. 2017). green valley galaxies have therefore long been thought of as the “crossroads” of galaxy evolution, a transitional population between the two main galactic stages of the star-forming blue cloud and the “red & dead” sequence (Bell et al. 2004; Martin et al. 2007; Faber et al. 2007; Mendez et al. 2011; Schawinski et al. 2014; Pan et al. 2015; Graham 2019), however, it is possible that these are also red sequence galaxies that have been rejuvenated (Graham et al. 2015, 2017).

The intermediate colours of these green valley galaxies have been interpreted as evidence for recent quenching (suppression) of star formation (Salim et al. 2007; Salim 2015; Smethurst et al. 2015; Phillipps et al. 2019). Star-forming galaxies are observed to lie on a well defined stellar mass-SFR relation (Martin et al. 2005), however, quenching a galaxy causes it to depart from this relation (Noeske et al. 2007; Peng et al. 2010). The main mechanism for galaxy quenching is thought to be a lack of fuel for star formation. Fading of the star-forming disc, the primary site of star formation, drives the apparent morphological transition of galaxies from spiral to lenticular or elliptical in the galaxies that are quenching and lie in the green valley (Coenda et al. 2018; Bluck et al. 2020; Fraser-McKelvie et al. 2019, 2020a,b).

Kelvin et al. (2018) examined 472 galaxies in the Galaxy And Mass Assembly (GAMA) survey with SDSS imaging visually for signs of disc substructures (e.g., rings, bars, and lenses) with a team of expert classifiers. They found evidence that rings and lenses are more common in the green valley than in red sequence and blue cloud galaxies. Our goal here is to re-examine this result using the GZ morphological estimates using the higher resolution and deeper Kilo-Degree Survey (KiDS) images (Kuijken et al. 2019) of the galaxies in the GAMA survey’s equatorial fields (Driver et al. 2011). Our sample is of similar size as that of Kelvin et al. (2018) (396 vs 472) and there is likely overlap. There are two critical differences: the method of classification and the quality of the data. Our classifications are based on much improved data and arrived at with citizen science voting rather than a small expert panel. Our aim is to examine if the different data and classification schemes arrive at qualitatively the same conclusions for the morphology of the green valley.

Our paper is organized as follows: Section 2 describes the GAMA and GZ data we use here, Section 3 presents our results and we discuss these in Section 4. Section 5 lists our conclusions.

2 DATA

In this paper, we use GAMA and Galaxy Zoo voting data based of the KiDS imaging.

¹ The red sequence was originally known as the color-magnitude relation for early-type galaxies, see the review in Graham (2013).

2.1 GAMA

The GAMA survey is a spectroscopic survey comprised of three equatorial fields and two Southern fields. Its multi-wavelength photometry ranges from ultraviolet to sub-mm wavelengths (Driver et al. 2009; Hopkins et al. 2013; Liske et al. 2015). Redshifts (z) are reliably found to $z \sim 0.8$ and the survey is complete to $\sim 98\%$ for an apparent magnitude in Sloan Digital Sky Survey r -filter (SDSS- r) of 19.8 mag in the equatorial fields. Here, we consider only these (G09, G12 and G15), as they overlap with the KiDS (KiDS de Jong et al. 2013, 2015, 2017; Kuijken et al. 2019), on which the GZ information is based (see next section).

We use GAMA optical photometry from SDSS Stripe-82 photometry Taylor et al. (2011), which is corrected for redshift (K-correction) and internal dust extinction. The final photometry we used is the LAMBDAR photometry (v01) presented in Wright et al. (2017).

Separately, we use stellar masses derived from the spectral energy distribution (SED) model fit using MAGPHYS tool (da Cunha et al. 2008), presented in Driver et al. (2016); Wright et al. (2017) (v06 in DR3).

2.2 KiDS GZ

The GZ citizen science project analyzed KiDS (de Jong et al. 2013, 2015, 2017; Kuijken et al. 2019) images. Citizen scientists answered a series of questions based on KiDS g-band and r-band imaging. A synthetic green channel was constructed as the arithmetic mean of the other two to allow for the construction of three-colour RGB images. Because morphological detail is lost with distance, a limit of $z \leq 0.075$ is enforced to ensure reliable morphological estimates of kpc-scale structures (e.g. spiral arms, bars). Initially we ran this data with a $z \leq 0.15$, however, we realized limitations in the Galaxy Zoo data that limited us to $z \leq 0.08$ making resolution for many morphological structures difficult. Therefore, we decided on our sample to $z \leq 0.075$ to limit the bias due to distance effects in the Galaxy Zoo voting.

The GZ question tree is presented in Holwerda et al. (2019) and in Figure 1. The full Galaxy Zoo classification is described in Kelvin et al. (*in preparation*). We focus on the questions that are asked in the GZ question tree (Figure 1) regarding disc galaxy morphology. In section 3, we begin each subsection with the question code and associated question of the morphological features as asked in the GZ questionnaire. These question codes are T00, T01, T02, T03, T04, T05, T06, T09 and T10. We refer the reader to Kelvin et al. (*in preparation*) for specific details of the GZ analysis. We used an internal GAMA/KiDS catalogue for the subsequent analysis.

2.3 Sample selection

We organized our GZ data by stellar mass, $\log(M_*/M_\odot)$, vs. intrinsic stellar population colour plane ($u^* - r^*$) (the population selections are from Bremer et al. 2018). Figure 2 shows our selection of blue cloud, green valley, and red sequence galaxies, based on their stellar mass and rest-frame colour. A second requirement is that these galaxies are disc-dominated following the T00 question (Figure 1) “Is the galaxy in the centre of the image simply smooth and rounded or does it have features?” with any fraction of the votes in favor of any features ($f_{features} > 0$). This is to remove any galaxies without features to further examine.

For the first graph in Figure 2 we limited the mass to $10.25 < \log(M_*/M_\odot) < 10.75$ and a redshift of $z \leq 0.075$. This mass range was selected to ensure a complete sample and for a more direct comparison with Kelvin et al. (2018), who select galaxies in the same

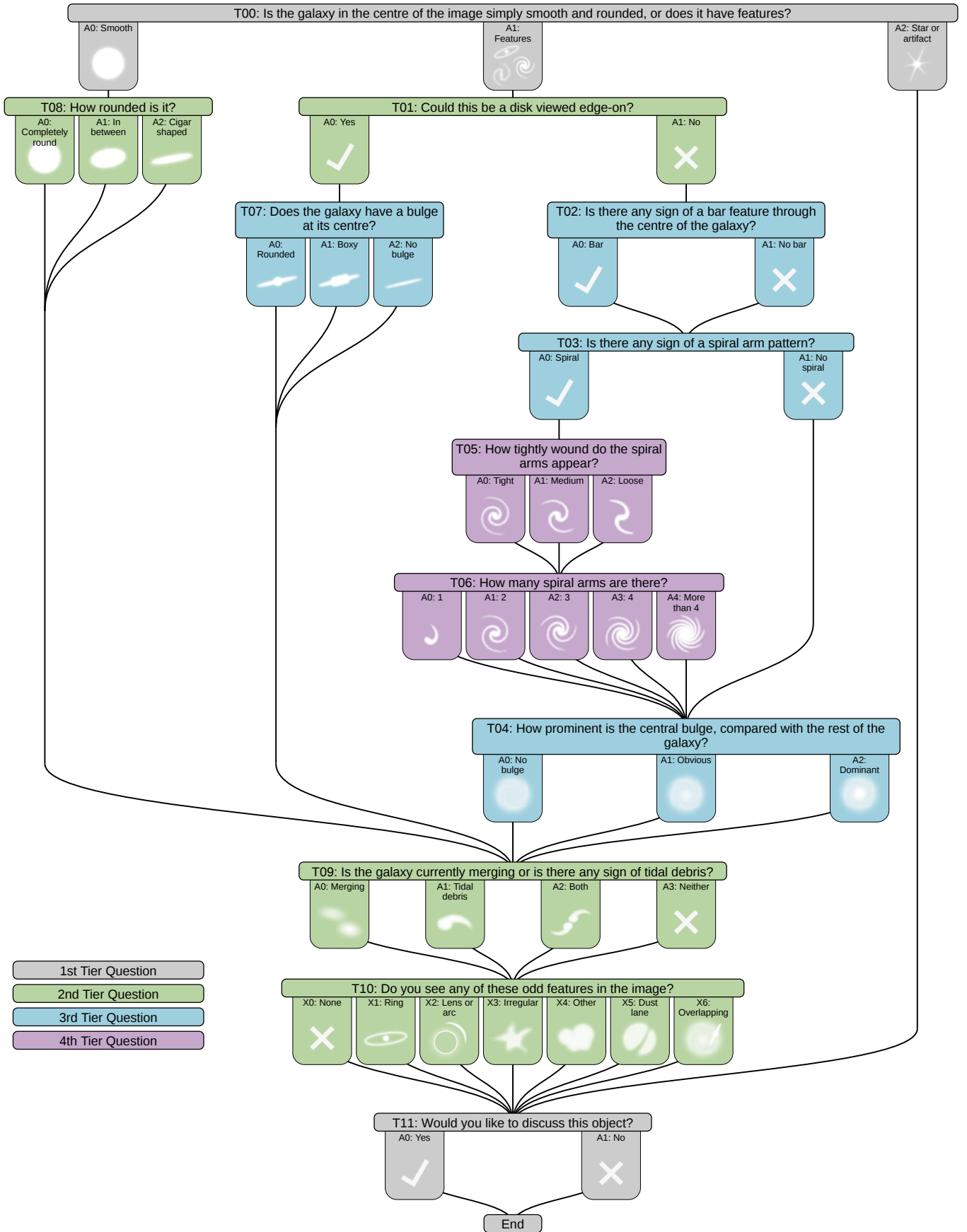


Figure 1. The flow diagram of the GZ4 (fourth generation) question tree. We refer to the text for details on the questions in the GAMA sample.

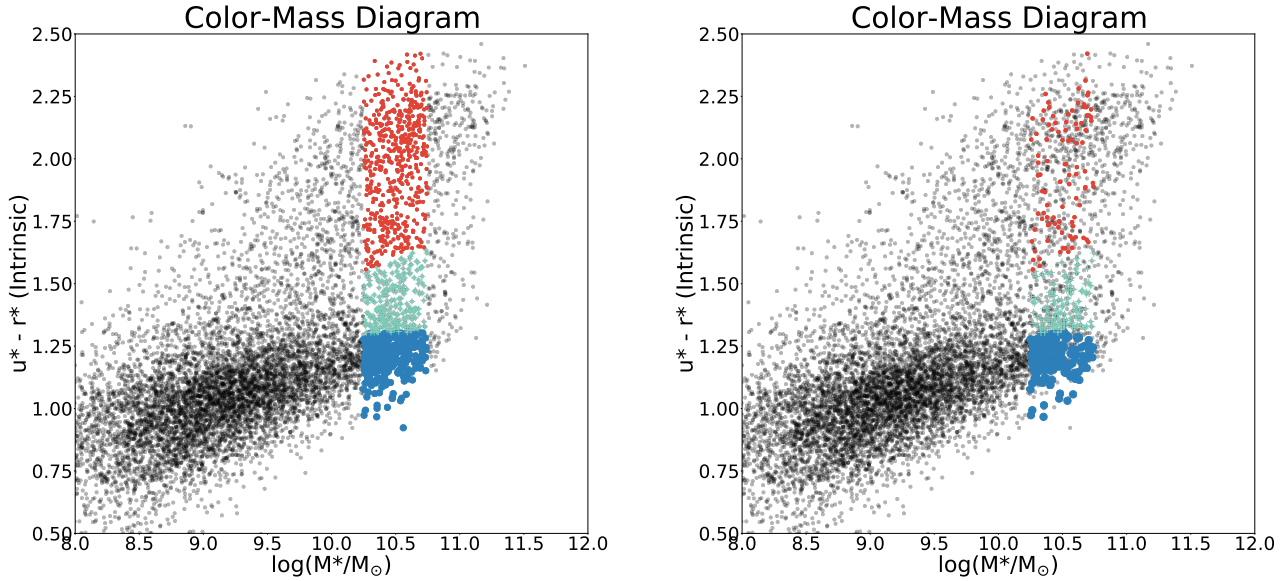


Figure 2. These plots represent all the GAMA galaxies in our mass range ($10.25 < \log(M_*/M_\odot) < 10.75$) colour -coded for their classification. We use the limits from [Bremer et al. \(2018\)](#) to select red, green and blue galaxies. The left panel represents all the respective galaxies in their mass ranges before further data selection. The right panel shows all galaxies with any votes between .1 and 1 for not being seen edge on and votes between .3 and 1 for spiral features. The right image represents our current data selection.

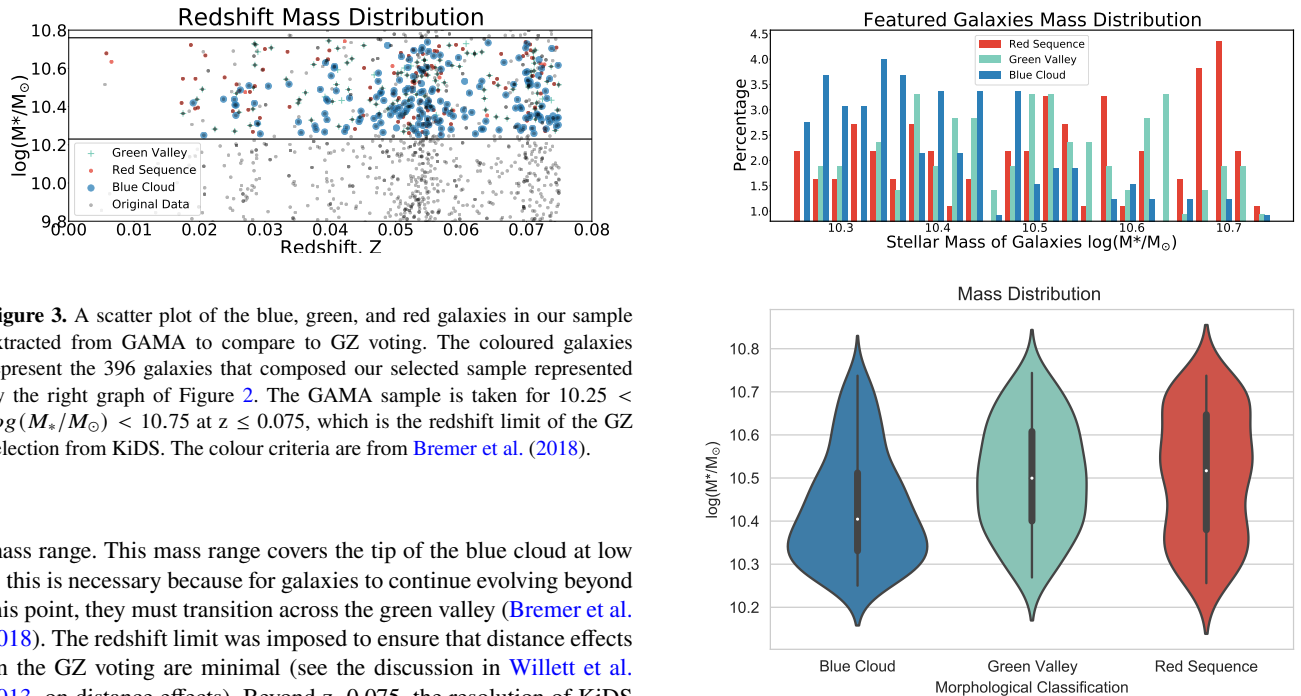


Figure 3. A scatter plot of the blue, green, and red galaxies in our sample extracted from GAMA to compare to GZ voting. The coloured galaxies represent the 396 galaxies that composed our selected sample represented by the right graph of Figure 2. The GAMA sample is taken for $10.25 < \log(M_*/M_\odot) < 10.75$ at $z \leq 0.075$, which is the redshift limit of the GZ selection from KiDS. The colour criteria are from [Bremer et al. \(2018\)](#).

mass range. This mass range covers the tip of the blue cloud at low z , this is necessary because for galaxies to continue evolving beyond this point, they must transition across the green valley ([Bremer et al. 2018](#)). The redshift limit was imposed to ensure that distance effects on the GZ voting are minimal (see the discussion in [Willett et al. 2013](#), on distance effects). Beyond $z=0.075$, the resolution of KiDS images is not sufficient to discriminate features of a kiloparsec in scale, such as the width of spiral arms and rings. The voting can be corrected using debiasing but the GAMA dataset may be too small for that (but the Galaxy Zoo v4 will be).

The right graph of Figure 2 represents the galaxies in each faction that are voted in the GZ to have any votes for “Could this be a disc viewed edge on” as no and “Is there any sign of a spiral arm pattern?” that registered 30% or higher. (T01 and T03 in the Figure 1 respectively). To do this, we set the voting for T01 results to fraction

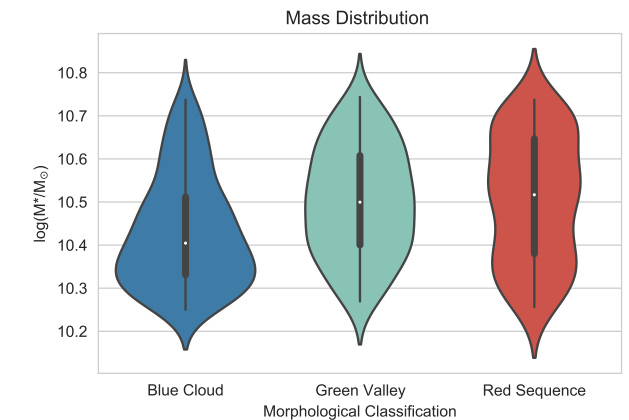


Figure 4. A histogram of the blue, green, and red galaxies in our selection sample (right graph of Figure 2) extracted from GAMA to compare with GZ voting. The GAMA sample is taken for ($10.25 < \log(M_*/M_\odot) < 10.75$) and $z \leq 0.15$, the limit of the GZ selection from KiDS. The histogram illuminates the overlap of data presented in Figure 3. The violin plot below shows the same information as in the histogram above it.

limits between 0.0001 and 0.9999 to prevent the possible error of galaxies with single votes throwing off the results, and to maximize those votes for features. We continued to do the same with T02, however this time we set the limits between .3 and 1. This allowed us to choose galaxies that had votes for bulges, spiral features and all other morphological features down this branch of the questionnaire. Lastly for this step we limited our selection for spiral features in the same way. We were left with a data set of 176 for blue cloud, 118 for green valley, and 102 for red sequence for the total of 396 in the mass range considered.

Figure 3 shows the distribution of featured galaxies in redshift (z) and stellar mass (M_*). Our selection is made to the specifications of $10.25 < \log(M_*/M_\odot) < 10.75$ and $z \leq 0.075$, the redshift limit of GZ pre-selection for classification. This gives us a good representative volume to compare galaxy morphology. We find that red sequence galaxies are at slightly higher masses than the blue cloud, with the green valley galaxies spanning an intermediate mass range. The galaxy spread is better represented by mass in Figure 4.

3 RESULTS

We compared the normalized fractions of galaxies between the blue cloud, green valley, and red sequence galaxies to generate the voting histograms and violin plots showing sample fractions in the following subsections.

As shown in Figure 1, each tier signified with a code, T##. This code represents question asked in the GZ about a morphological trait with the number denoting the tier of each question. We organized each subsection by these question codes with their represented data in a histogram.

The tool used to compare these data is the Kolmogorov-Smirnov (K-S) two-sample similarity test and the associated p-value calculated for our selection samples. The K-S value provides the maximum difference between any 2 cumulative distributions we consider. The p-value is the probability of the random occurrence of the presented null hypothesis (the distributions are the same).

We plot the voting in the Galaxy Zoo in two ways in each of the following Figures. In the top panel, we plot the cumulative histogram of the voting in Galaxy Zoo: on the x-axis is the fraction of voting in favor of the question under consideration and on the y-axis the fraction of the sample is shown. A plot that rises early has a larger fraction of the sample with a low fraction of the votes in favor of this feature being present. In this case, the feature is relatively rare. If the plot rises on the right of the x-axis, a large fraction of the sample has a high fraction of votes (or greater consensus) that this feature is present.

In the lower panel we present the same fraction of the voting in a more traditional histogram, rendered as a violin plot (a mirrored histogram with a kernel density applied to render it into a smooth graph). Because the distribution is slightly smoothed, the range of values in the y-axes in the Figures goes from -0.2 to 1.2 to accommodate the tails resulting from the kernel smoothing. The range and standard deviations of the distribution are also shown as thin and thick horizontal lines.

By combining both graphical visualizations in each plot, we hope to show both when voting behaviour between populations is similar or dissimilar in the cumulative distribution, reflected in the K-S metric, and how the voting behavior looks in each population in a more intuitive histogram rendering.

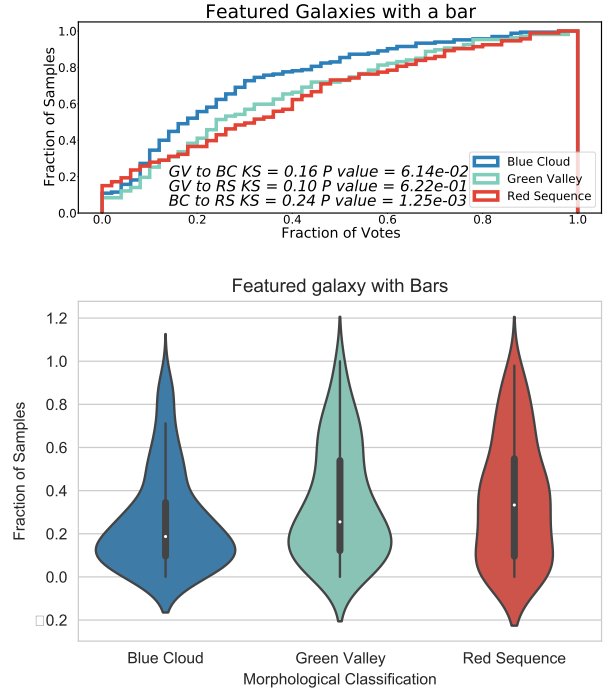


Figure 5. A histogram of the fraction of votes in favor of classifying galaxies as featured with a bar (T02 in the GZ questionnaire). The difference between the 3 groups is nearly equally as distinguishable with K-S values of 0.16 for green valley and blue cloud, 0.10 for green valley and red sequence, and 0.24 for blue cloud and red sequence. The significance from p-values is 6.14×10^{-02} , 6.22×10^{-01} , and 1.25×10^{-03} respectively. This confirms that the 3 groups are statistically variant. The violin plots represent the same data

3.1 Bars

Figure 1, T02: “Is there a sign of a bar feature through the centre of the galaxy?”

Stellar bars are a prime suspect for a morphological feature that aids in quenching, especially quenching from the inside-out (see Masters et al. 2021, for a review).

GZ voting show that red sequence and green valley have a lower fraction of galaxies having bar shaped structures than blue cloud. In our statistical analysis, we have chosen to only include galaxies that were voted as bar galaxies 50 % ($f_{bar} > 0.5$) or more of the time. From our galaxy sample for each faction, 12.1% of blue cloud, 20.1% of green valley, and 19.3% of red sequence galaxies met this requirement. These percentages are to be expected if the green valley is a transition zone and bars are in fact a predecessor to quenching and long-lived enough to do so. Figure 5 shows the similar voting behaviour in Galaxy Zoo in the red sequence and green valley. The notably different behaviour in the blue cloud shows lower confidence in more of the blue cloud sample of galaxies.

3.2 Featured discs

Figure 1, T03: “Is there any sign of a spiral arm pattern?”

Using the voting data from this question showed the galaxies with spiral features in the red sequence, blue cloud, and green valley.

The outcome, as shown in Figure 6, shows that most disc galaxies in the blue cloud are featured galaxies. There are fewer featured galaxies among the disc galaxies of the red sequence. The number

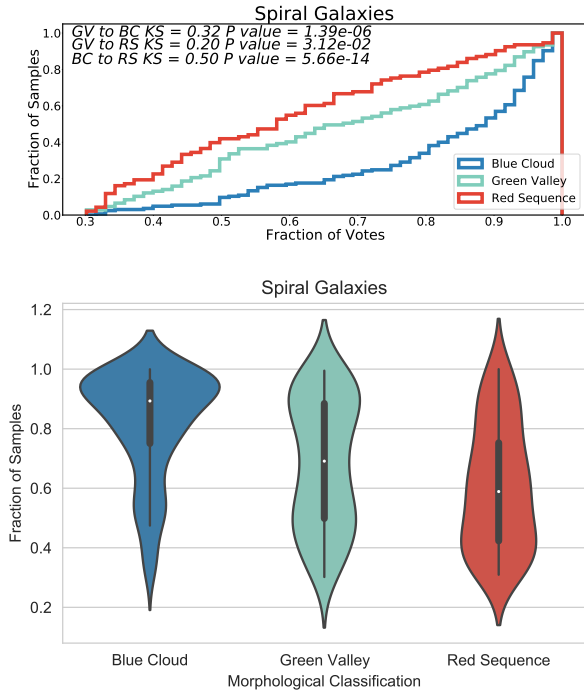


Figure 6. A histogram of the fraction of votes in favor of classifying galaxies as featured (T00 in the GZ questionnaire). According to the K-S test, the difference between the green valley and blue cloud is very distinguishable with a value of 0.37. The difference between green valley and red sequence is distinguishable as well, with a KS value of 0.20. The difference between blue cloud and red sequence results from a KS value of 0.50. These differences are further confirmed due to very small p-values. They are 1.39×10^{-06} , 3.12×10^{-02} , 5.66×10^{-14} respectively. The violin plots represent the same data as the cumulative histogram at the top.

of featured galaxies in the green valley falls somewhere in between those present in the blue cloud and red sequence. The fractions of galaxies with discs is possibly an under-estimate as lenticular galaxies are often missed in visual inspections (Graham 2019).

3.3 Winding of Spiral Arms

Figure 1, T05: “How tightly wound do the spiral arms appear?”

Green valley galaxies tend to follow the blue cloud in behaviour in spiral arm winding of tight and medium, but lead in voting of loose winding. red sequence continues to show the opposite behaviour of the blue cloud (see, for example, Figures 7,8,and 9).

Since T05 is a choice between these three questions and one cannot progress without clicking one option, the plots in Figures 7,8,and 9 are complementary. It shows that loose winding is preferred for blue cloud and tight winding for the red sequence and the green valley voting behaviour is somewhere in between. It also shows that the “medium” option voting is much more similar for all three populations as a compromise option but remains less of a preference for the red sequence galaxies, strongly suggesting that red sequence galaxies have tightly wound arms.

3.4 Number of Spiral Arms

Figure 1, T06: “How many spiral arms are there?”

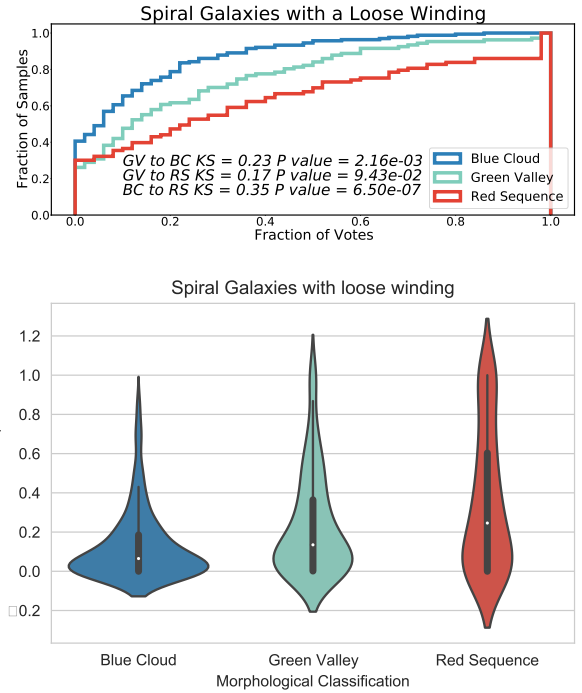


Figure 7. Histogram of the fraction of votes in favor of the spiral galaxies having a Loose winding (T05 in the GZ questionnaire). The difference between green valley and blue cloud galaxies is distinguishable with a KS of 0.23, the KS of green valley and red sequence is 0.17, and the KS of the blue cloud and red sequence is 0.35. green valley to blue cloud is at a p value 2.16×10^{-03} , green valley and red sequence is 9.43×10^{-02} , and the KS of red sequence and blue cloud is 6.5×10^{-07} . The violin plots in the lower panel represent the same data as the cumulative histogram at the top.

Green valley galaxies are more symmetric (180° rotationally symmetric), as the higher relative voting fraction points out. They are favored to have 2 arms, rather than 1 or 3 (which may be 120° symmetric). Spiral galaxies with an odd number of arms are more commonly found in the blue cloud, the voting suggests (see, for example, Figure 10). The number of arms have been linked to specific star-formation decline (Porter-Temple et al. submitted) and the relative distribution of voting for 3-armed spirals in the red sequence, green valley and blue cloud reflect this.

3.5 Central Bulge Prominence

Figure 1, T04: “How prominent is the central bulge, compared with the rest of the galaxy?”

Figure 11 shows the voting behaviour for this question with the highest voting fractions, i.e. largest fraction of the sample with high voting confidence, for a dominant bulge in the red sequence, followed by green valley and blue cloud. This trend is an expected result following the current understanding of galaxy evolution from green valley to red sequence i.e discs fading and turning red and the bulge gaining relative prominence with respect to the disc.

3.6 Rings

Figure 1, T10: “Do you see any of these odd features in the image?”

This last question in the question tree of the Galaxy Zoo (Figure 1) is for citizen scientist to identify rarer morphological phenomena,

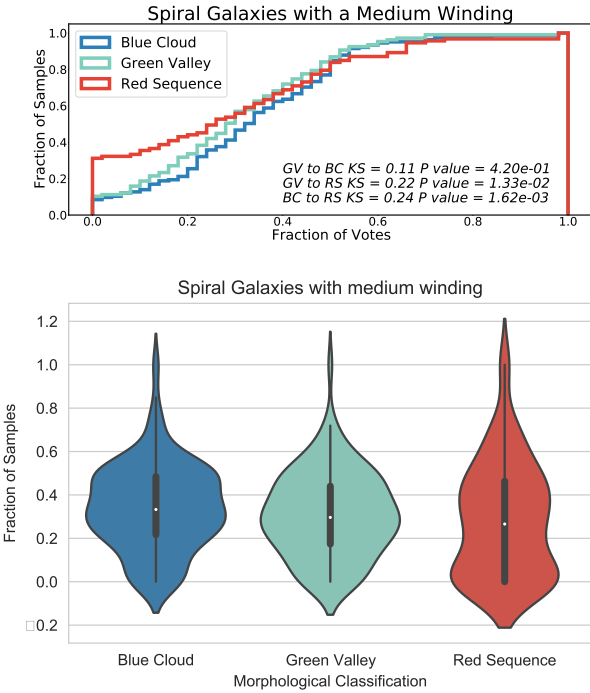


Figure 8. Histogram of the fraction of votes in favor of the spiral galaxies having a Medium winding (T05 in the GZ questionnaire). The difference between green valley and blue cloud is distinguishable with a KS of 0.11, but the difference between the green valley and red sequence is Distinguishable at a KS value of 0.22, and the largest difference is between the behaviour of the red sequence and the blue cloud with a KS of 0.24. The Significance of these results are green valley to blue cloud with p value 4.2×10^{-01} , green valley to red sequence with 1.33×10^{-02} , and blue cloud to red sequence with 1.61×10^{-03} . This shows again how the behaviours of the blue cloud and red sequence are opposite with green valley maintaining the middle. The violin plots represent the same data as the cumulative histogram in the top panel.

which are expected to be rare, such as accidental overlaps of galaxies along the line-of-sight (see Keel et al. 2013; Holwerda 2017, for a discussion on these). One of the options is to identify a ring, as opposed to a lensing object, as this odd feature.

Though the source of rings is still heavily debated, the abundance of inside quenching may be a potential cause (Kelvin et al. 2018). We expect a direct correlation between the presence of bars and rings in featured galaxies if the inside-out quenching theory holds true. We see this behaviour in the blue cloud and the red sequence (steady increase in bars in disc galaxies from blue cloud to red sequence, Figure 5). However, there is an even stronger prevalence of ring galaxies in the green valley (Figure 12). This could be a sign of increased inside quenching or ring formation in the green valley, driven by other possible factors.

4 DISCUSSION

The transition of galaxies from the star-forming blue cloud to the passive red sequence through the green valley is thought to be from a variety of processes, both internal and external and can be in either direction (see Salim 2015, for a review). There appears to be a relation between galaxy morphology and their transition speed (Schawinski et al. 2014; Smethurst et al. 2015); smooth galaxies undergo a rapid transit through major mergers, intermediate complex

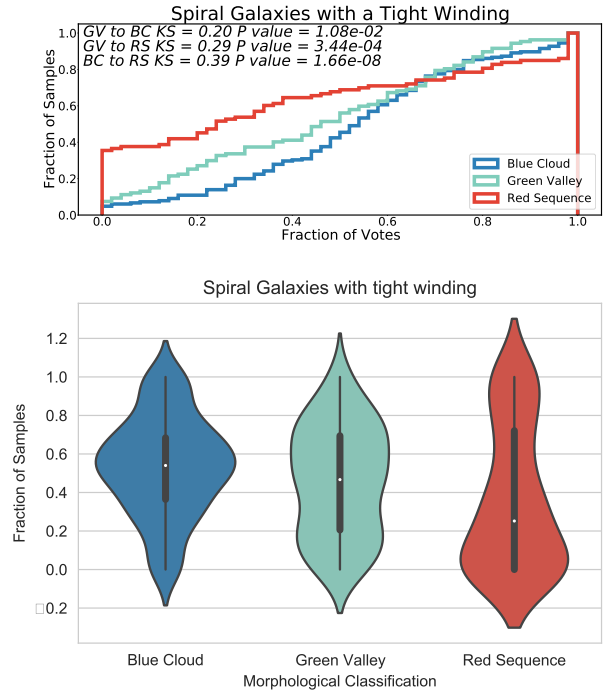


Figure 9. Histogram of the fraction of votes in favor of the spiral galaxies having a tight winding (T05 in the GZ questionnaire). The difference between green valley and blue cloud is distinguishable with a KS of 0.20, but the difference between the green valley and red sequence is 0.29 with the difference between the red sequence and blue cloud being the most distinguishable at 0.39. The significance of these are represented with the p-values of green valley and blue cloud at 1.08×10^{-02} , green valley and red sequence at 3.44×10^{-04} , and blue cloud and red sequence at 1.66×10^{-08} . The violin plots represent the same data as the top panel histograms.

galaxies (e.g. S0) undergo minor mergers and galaxy interactions for an intermediate crossing scale, and disc galaxies cross the slowest due to secular processes. In disc galaxies, bars and bulges suspected to play a role in the quenching process (Nogueira-Cavalcante et al. 2017; Gu et al. 2018; Ge et al. 2018; Kelvin et al. 2018). Green valley quenching appears to be ongoing since $z \sim 2$ (Jian et al. 2020) with a mass-dependence on transition speed and phase (Schawinski et al. 2014; Anghopo et al. 2020). Higher mass galaxies appear to quench mostly due to lack of gas supply (Das et al. 2021) and quenching does seem linked to a lack of Circumgalactic Medium (CGM) (Kacprzak et al. 2021). At lower masses, morphological features are thought to influence the quenching speed (Smethurst et al. 2015), motivating our morphological characterization of green valley galaxies.

Citizen scientists were asked if the galaxies they were looking at were ring galaxies. We have analyzed the Galaxy Zoo votes of galaxies of a mass ($10.25 < \log(M_*/M_\odot) < 10.75$), as was done in Kelvin et al. (2018). However, we increased the redshift from $z < 0.06$ to $z < 0.075$ thanks to the improved resolution of the KiDS images. This larger sample size gave us very similar overall results to those from Kelvin et al. (2018), i.e. a higher fraction of ring galaxies in green valley featured galaxies. The data presented in Figure 12 demonstrates this behaviour. Initially, we had constrained our sample to $z < 0.15$, the full redshift range of GAMA/GZ data. The results were qualitatively similar but distance effects cannot be fully ruled out and we imposed the $z = 0.075$ limit (the distance KiDS resolution corresponds to a 1 kpc feature).

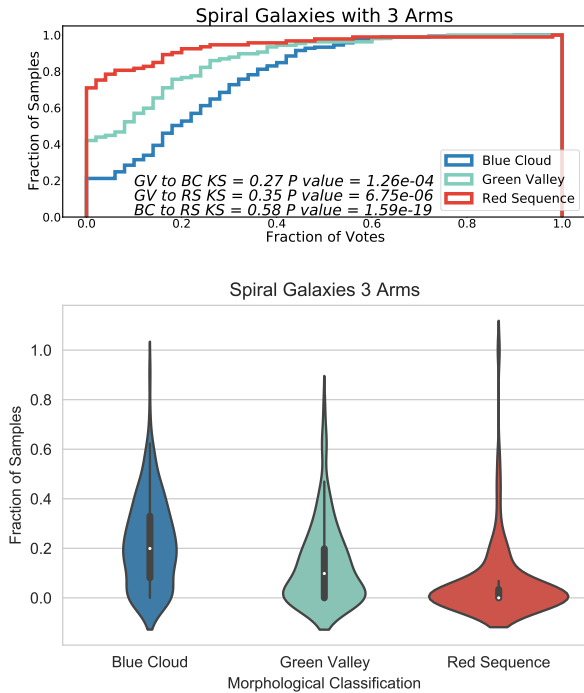


Figure 10. A histogram of the fraction of votes in favor of classifying the galaxies as spiral with 3 arms (T10 in the GZ questionnaire). The difference between the green valley and blue cloud is very distinguishable with a K-S value of 0.27. green valley to red sequence is distinguishable with a K-S value of 0.35. The highest difference is seen between blue cloud and red sequence with a K-S of 0.58. The significance from p-values is 1.26×10^{-04} , 6.75×10^{-06} , and 1.59×10^{-19} respectively. This shows that spiral galaxies with 3 arms are found more frequent in the blue cloud and green valley. The violin plots represent the same data

It is clear that the green valley has a higher concentration of ring featured galaxies than both the red sequence and the blue cloud. This is not the only example of green valley exhibiting its own behaviour, as explained in section 3.3, green valley have an initial behaviour of looser arm windings (Figure 7). We have also shown that the red sequence and green valley have higher concentrations of featured galaxies with bars while the blue cloud possesses the lowest amount of featured galaxies with bars (Figure 5). Earlier studies found that barred galaxies may transition slower (Nogueira-Cavalcante et al. 2017) or that bulges play a role in the transition through the green valley (Ge et al. 2018), some of whom may be rejuvenating rather than quenching (Mancini et al. 2019).

As previously stated, it is theorized that quenching may cause ring formation. The existence of bars may expedite the quenching process, which may in turn lead to faster ring formation. This shows a possible link between the role bars and rings in galaxy quenching. The green valley represented in the histogram in Figure 5 shows a difference in behaviour than seen with rings in Figure 12. The voting for bars in green valley galaxies in Figure 5 is in between the voting for blue cloud and red sequence. The voting in green valley in Figure 12 is more confident in a rings than either the blue cloud or the red sequence; a larger fraction of the green valley sample has a higher confidence in rings than either comparison sample.

However, by looking at our violin graphs portion of Figure 12, we see that the distribution of the green valley galaxy sample is spread over the whole range of possible values (galaxies with high

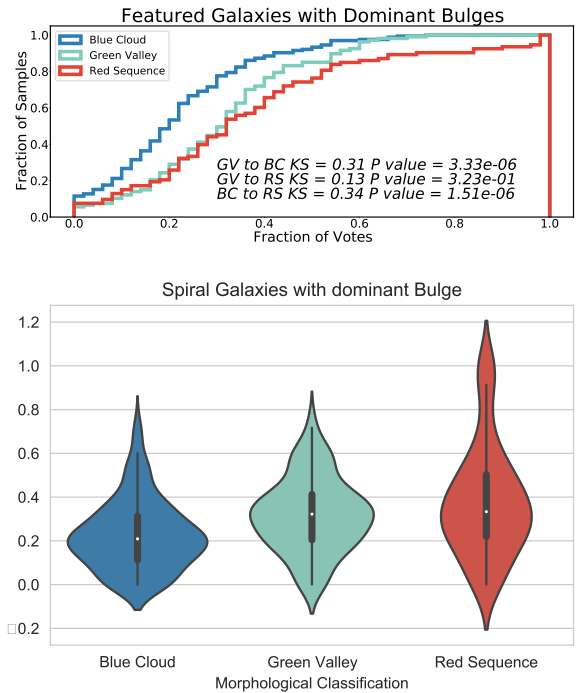


Figure 11. A histogram of the fraction of votes classifying disc galaxies with dominant bulges (T04 in the GZ questionnaire). The difference between the green valley and blue cloud is distinguishable with a K-S of 0.31. This difference is less distinguishable between the green valley and the red sequence, with a K-S value of 0.13. When comparing the blue cloud to the red sequence, the K-S value is 0.34. The significance p-values are 3.33×10^{-06} , 3.23×10^{-01} , and 7.55×10^{-03} respectively.

and low confidence in a ring) while the blue cloud galaxies are mostly clustered at low confidence in rings while the red sequence galaxies resemble a high confidence and a low confidence population. The green valley resemble the red sequence but with higher voting fractions.

This could be due to the fact that this is a transition zone and the younger green valley galaxies have yet to exhibit the bar or ring behaviours that may occur later in their lifetimes in the green valley, just before entering the red sequence. Future studies with even more Galaxy Zoo information will help probe the link between bar and ring formation and the green valley population.

Furthermore, we studied the possibility of a correlation between Dominant bulges and rings (Figures 11 and 12 respectively). Though it does appear that the green valley is in the middle in both the bulge and ring distributions, the role of internal quenching remains unclear. It is not clear why a fading disc will result in either a ring or a tightening of the spiral arm. Perhaps, over time, the reduction of gas in the disc results in a lower density for the spiral density wave (e.g. Roberts et al. 1975; Dobbs & Baba 2014; Shu 2016) and thus a different spiral pattern speed. This change in the spiral density wave could lead to either a tightening of the spiral arms or ring formation. This depends however on the dominant formation mechanism for spiral arms (Davis et al. 2019). Rings could quench the disc or the quenching of the disc could form rings.

When all conditions are carefully considered, the preference for green valley galaxies to be classified with rings suggests that any quenching in the green valley is accompanied by subtle changes in disc morphology as well as mere dimming of the disc.

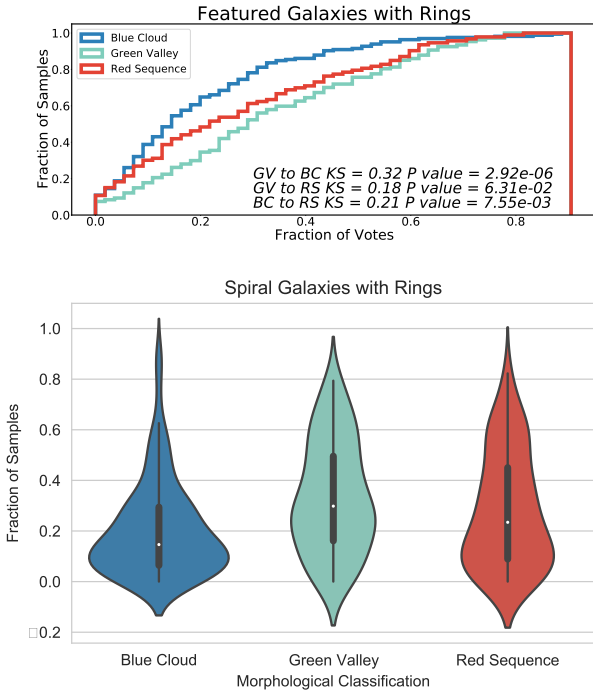


Figure 12. A histogram of the fraction of votes labeling galaxies as featured with rings (T06 in the GZ questionnaire). The green valley is distinguishable from the blue cloud with a K-S value of 0.32. The green valley continues to differ from the red sequence with a K-S value of 0.18; while the red sequence to blue cloud difference has a K-S value of 0.21. The significance p-values are 2.92×10^{-06} , 6.31×10^{-02} , and 7.55×10^{-03} respectively. This is the first time we observe a difference in the location of the green valley data. Here, it is no longer in between the blue cloud and the red sequence, thus presenting behaviour of its own.

5 CONCLUSIONS

We find that the red sequence leads in highest concentration of featured galaxies with bulges. It is followed by the green valley (Figure 11). A lack of new-forming stars in the red sequence leads to a lack of contrast, which may allow bulges to be more visible. This is the diametrically opposite case to bulges in the blue cloud.

Our results match Galaxy Zoo voting (on KiDS images) in confirming that green valley featured galaxies have the most rings in comparison to their blue cloud and red sequence counterparts (Figure 12). This confirms the initial prominence of rings in green valley galaxies found by Kelvin et al. (2018).

Our findings also show a gradual loosening of spiral arms as galaxies enter the green valley. blue cloud galaxies are viewed predominantly with tightly wound arms, while every kind of spiral arm winding is present in the red sequence. A trend is visible in the voting on central bulge prominence; bulges become more dominant from blue cloud to red sequence, with the green valley displaying an intermediate distribution.

Our thorough study of galaxies classified in the green valley indicates that their behaviours typically share characteristics with both the red sequence and blue cloud, placing it in the middle (Figure 6), thereby highlighting the transitional interstitial nature of the green valley.

6 DATA AVAILABILITY

This work is predominantly based on public data from the GAMA survey (available at <http://www.gama-survey.org/dr3/>) and the Galaxy Zoo catalogue for the GAMA fields, to be released with DR4 (Driver et al. *in prep.*)

ACKNOWLEDGEMENTS

The material is supported by NASA Kentucky award No: 80NSSC20M0047 (NASA-REU to L. Habertzettl and D. Smith). D. Smith would like to thank C Nasr for her assistance.

This publication has been made possible by the participation of all the volunteers in the Galaxy Zoo project. Their contributions are individually acknowledged at <http://www.GalaxyZoo.org/Volunteers.aspx>.

REFERENCES

- Anghojo J., Ferreras I., Silk J., 2020, MNRAS, 495, 2720
 Arnouts S., et al., 2007, A&A, 476, 137
 Baldry I. K., Glazebrook K., Brinkmann J., Ivezić Ž., Lupton R. H., Nichol R. C., Szalay A. S., 2004, ApJ, 600, 681
 Baldry I. K., Balogh M. L., Bower R. G., Glazebrook K., Nichol R. C., Bamford S. P., Budavari T., 2006, MNRAS, 373, 469
 Ball N. M., Loveday J., Brunner R. J., 2008, MNRAS, 383, 907
 Bamford S. P., et al., 2009, MNRAS, 393, 1324
 Barone T. M., et al., 2022, MNRAS, 512, 3828
 Bell E. F., et al., 2004, ApJ, 600, L11
 Bluck A. F. L., et al., 2020, MNRAS, 499, 230
 Brammer G. B., et al., 2009, ApJ, 706, L173
 Bremer M. N., et al., 2018, MNRAS, 476, 12
 Coenda V., Martínez H. J., Muriel H., 2018, MNRAS, 473, 5617
 Corcho-Caballero P., Ascasibar Y., López-Sánchez Á. R., 2020, MNRAS, 499, 573
 Corcho-Caballero P., Casado J., Ascasibar Y., García-Benito R., 2021, MNRAS, 507, 5477
 Das A., Pandey B., Sarkar S., 2021, J. Cosmology Astropart. Phys., 2021, 045
 Davis B. L., Graham A. W., Combes F., 2019, ApJ, 877, 64
 Dobbs C., Baba J., 2014, PASA, 31, e035. doi:10.1017/pasa.2014.31
 Driver S. P., et al., 2006, MNRAS, 368, 414
 Driver S. P., et al., 2009, Astronomy and Geophysics, 50, 050000
 Driver S. P., et al., 2011, MNRAS, 413, 971
 Driver S. P., et al., 2016, ApJ, 827, 108
 Faber S. M., et al., 2007, ApJ, 665, 265
 Fraser-McKelvie A., et al., 2019, MNRAS, 488, L6
 Fraser-McKelvie A., et al., 2020a, MNRAS, 495, 4158
 Fraser-McKelvie A., et al., 2020b, MNRAS, 499, 1116
 Ge X., Gu Q.-S., Chen Y.-Y., Ding N., 2018, arXiv e-prints, p. arXiv:1808.01709
 Graham A. W., 2013, preprint
 Graham A. W., 2019, MNRAS, 487, 4995
 Graham M. L., Sand D. J., Zaritsky D., Pritchett C. J., 2015, preprint
 Graham A. W., Janz J., Penny S. J., Chilingarian I. V., Ciambur B. C., Forbes D. A., Davies R. L., 2017, ApJ, 840, 68
 Gu Y., Fang G., Yuan Q., Cai Z., Wang T., 2018, preprint
 Holwerda B., 2017, The Cluster Population of UGC 2885, HST Proposal
 Holwerda B. W., et al., 2019, AJ, 158, 103
 Hopkins A. M., et al., 2013, MNRAS, 430, 2047
 Jian H.-Y., et al., 2020, ApJ, 894, 125
 Kacprzak G. G., Nielsen N. M., Nateghi H., Churchill C. W., Pointon S. K., Nanayakkara T., Muzahid S., Charlton J. C., 2021, MNRAS, 500, 2289
 Keel W. C., Manning A. M., Holwerda B. W., Mezzoprete M., Lintott C. J., Schawinski K., Gay P., Masters K. L., 2013, PASP, 125, 2

- Kelvin L. S., et al., 2018, MNRAS, 477, 4116
Kuijken K., et al., 2019, A&A, 625, A2
Lintott C. J., et al., 2008, MNRAS, 389, 1179
Liske J., et al., 2015, MNRAS, 452, 2087
Mancini C., et al., 2019, MNRAS, 489, 1265
Martin D. C., et al., 2005, ApJ, 619, L1
Martin D. C., et al., 2007, ApJS, 173, 342
Masters K. L., et al., 2010, MNRAS, 404, 792
Masters K. L., et al., 2021, MNRAS, 507, 3923
Mendez A. J., Coil A. L., Lotz J., Salim S., Moustakas J., Simard L., 2011, ApJ, 736, 110
Noeske K. G., et al., 2007, ApJ, 660, L43
Nogueira-Cavalcante J. P., Gonçalves T. S., Menéndez-Delmestre K., Sheth K., 2017, preprint
Pan Y. C., Sullivan M., Maguire K., Gal-Yam A., Hook I. M., Howell D. A., Nugent P. E., Mazzali P. A., 2015, MNRAS, 446, 354
Peng C. Y., Ho L. C., Impey C. D., Rix H., 2010, AJ, 139, 2097
Phillipps S., et al., 2019, MNRAS, 485, 5559
Roberts W. W. J., Roberts M. S., Shu F. H., 1975, ApJ, 196, 381
Salim S., 2015
Salim S., et al., 2007, ApJS, 173, 267
Schawinski K., 2009, MNRAS, 397, 717
Schawinski K., et al., 2007, ApJS, 173, 512
Schawinski K., et al., 2014, MNRAS, 440, 889
Shu F. H., 2016, ARA&A, 54, 667
Skibba R. A., et al., 2009, MNRAS, 399, 966
Smethurst R. J., et al., 2015, MNRAS, 450, 435
Smethurst R. J., Lintott C. J., Bamford S. P., Hart R. E., Kruk S. J., Masters K. L., Nichol R. C., Simmons B. D., 2017, MNRAS, 469, 3670
Strateva I., et al., 2001, AJ, 122, 1861
Taylor E. N., et al., 2011, MNRAS, 418, 1587
Taylor E. N., et al., 2015, MNRAS, 446, 2144
Willett K. W., et al., 2013, MNRAS, 435, 2835
Willmer C. N. A., et al., 2006, ApJ, 647, 853
Wright A. H., et al., 2017, MNRAS, 470, 283
da Cunha E., Charlot S., Elbaz D., 2008, MNRAS, 388, 1595
de Jong J. T. A., Verdoes Kleijn G. A., Kuijken K. H., Valentijn E. A., 2013, Experimental Astronomy, 35, 25
de Jong J. T. A., et al., 2015, A&A, 582, A62
de Jong J. T. A., et al., 2017, A&A, 604, A134

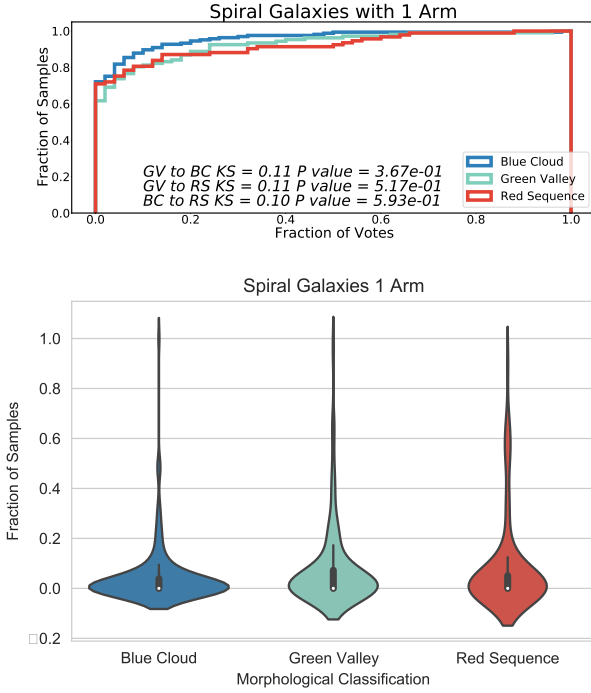


Figure A1. Histogram of the fraction of votes in favor of the galaxies having 1 Arm (T10 in the Galaxy Zoo questionnaire). The Difference between the green valley and blue cloud is not very distinguishable with a KS of 0.06, green valley is more distinguishable from the red sequence with a KS value of 0.12, keeping green valley between the behaviour of the red sequence and blue cloud that have the most difference with a KS value of 0.18. The significance between the green valley and blue cloud are 0.1, green valley to red sequence 4.18×10^{-05} , and blue cloud to red sequence 5.48×10^{-11} .

APPENDIX A: SUPPLEMENTAL FIGURES

In this section we supplied the histograms that were represented by the rest of the GAMA questions that were not in the main text.

This paper has been typeset from a $\text{\TeX}/\text{\LaTeX}$ file prepared by the author.

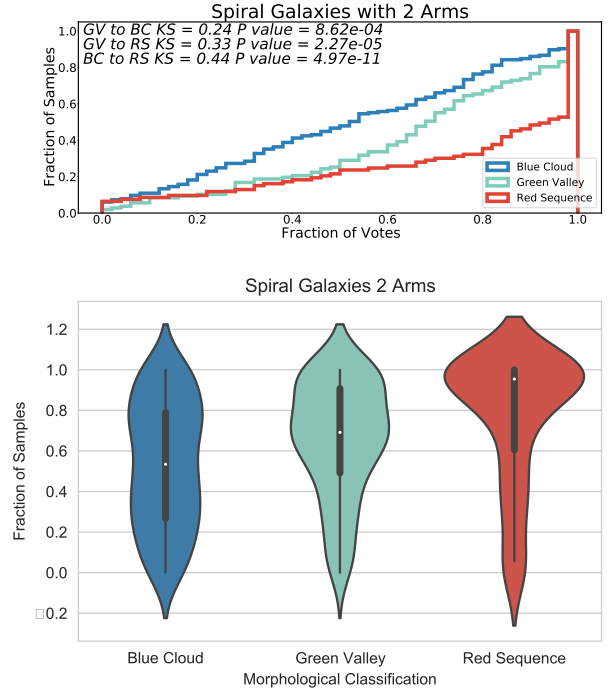


Figure A2. Histogram of the fraction of votes in favor of the galaxies having 2 Arms (T10 in the Galaxy Zoo questionnaire). The Difference between the green valley and blue cloud is distinguishable with a KS of 0.18, green valley is distinguishable from the red sequence with a KS value of 0.17 staying between the behaviour of the blue cloud and red sequence that have a KS of 0.33. The significance between the green valley and blue cloud are 1.14×10^{-10} , green valley to red sequence 1.93×10^{-09} , and blue cloud to red sequence 4.89×10^{-34} .

KS Values For Histograms			
Figure	green valley to blue cloud	green valley to red sequence	blue cloud to red sequence
5:Bars	0.16	0.10	0.24
6:Spiral	0.32	0.20	0.50
7:Loose	0.23	0.17	0.35
8:Medium	0.11	0.22	0.24
9:Tight	0.20	0.29	0.39
10:3 Arms	0.27	0.35	0.58
11:Dominate Bulge	0.31	0.13	0.34
12:Rings	0.32	0.18	0.21
A1:1 Arm	0.11	0.11	0.10
A2:2 Arm	0.24	0.33	0.44
A3:4 Arm	0.21	0.16	0.37
A4:4+ Arms	0.14	0.19	0.32
A5:Dust Lane	0.07	0.15	0.17
A6:Mergers	0.10	0.21	0.13
A7:Lenses or Arcs	0.14	0.14	0.07
A8:Tidal Debris	0.18	0.14	0.24
A9:Obvious Bulges	0.36	0.26	0.18

P Values For Histograms			
Figure	green valley to blue cloud	green valley to red sequence	blue cloud to red sequence
5:Bars	6.14×10^{-02}	6.22×10^{-01}	1.25×10^{-03}
6:Spiral	1.39×10^{-06}	3.12×10^{-02}	5.66×10^{-14}
7:Loose	2.16×10^{-03}	9.43×10^{-02}	6.50×10^{-07}
8:Medium	4.20×10^{-01}	1.33×10^{-02}	1.62×10^{-03}
9:Tight	1.08×10^{-02}	3.44×10^{-04}	1.66×10^{-08}
10:3 Arms	1.26×10^{-04}	6.75×10^{-06}	1.59×10^{-19}
11:Dominate Bulge	3.33×10^{-06}	3.23×10^{-01}	1.51×10^{-06}
12:Rings	2.92×10^{-06}	6.31×10^{-02}	7.55×10^{-03}
A1:1 Arm	3.67×10^{-01}	5.17×10^{-01}	5.93×10^{-01}
A2:2 Arm	8.62×10^{-04}	2.27×10^{-05}	4.97×10^{-11}
A3:4 Arm	6.77×10^{-03}	1.23×10^{-01}	9.97×10^{-08}
A4:4+ Arms	1.22×10^{-01}	5.23×10^{-02}	7.57×10^{-06}
A5:Dust Lane	9.07×10^{-01}	2.15×10^{-01}	4.62×10^{-02}
A6:Mergers	5.34×10^{-01}	1.81×10^{-02}	2.70×10^{-01}
A7:Lenses or Arcs	1.54×10^{-01}	2.76×10^{-01}	8.63×10^{-01}
A8:Tidal Debris	1.54×10^{-01}	5.64×10^{-02}	1.75×10^{-03}
A9:Obvious Bulges	2.19×10^{-04}	5.68×10^{-02}	3.12×10^{-07}

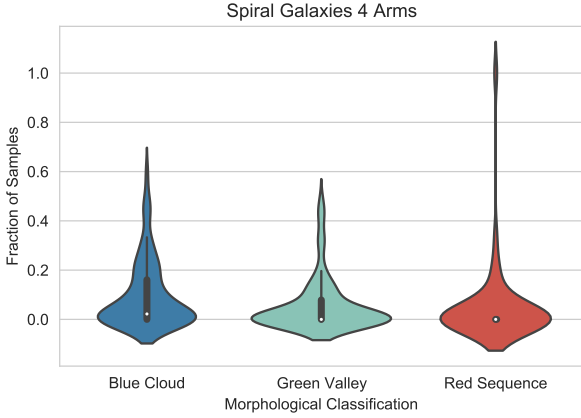
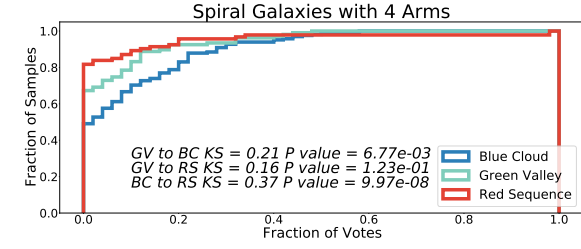


Figure A3. Histogram of the fraction of votes in favor of the galaxies having 4 Arms (T10 in the Galaxy Zoo questionnaire). The Difference between the green valley and blue cloud is distinguishable with a KS of 0.17, green valley is less distinguishable form the red sequence with a KS value of 0.06 staying between behaviour of the blue cloud and red sequence with a KS of 0.22. The significance between the green valley and blue cloud are 5.32×10^{-09} , green valley to red sequence 0.15, and blue cloud to red sequence 3.5×10^{-16} .

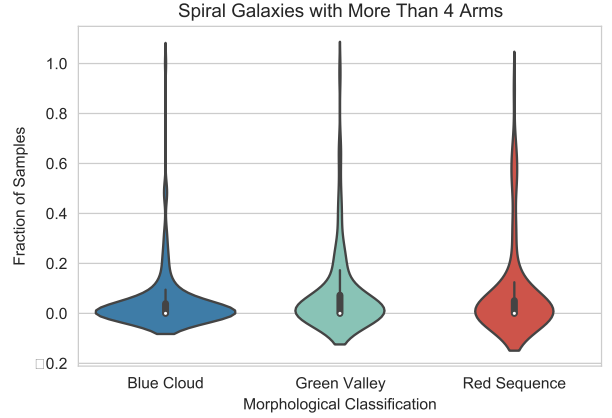
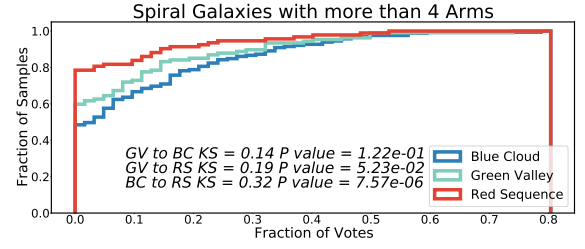


Figure A4. Histogram of the fraction of votes in favor of the galaxies having more than 4 Arms (T10 in the Galaxy Zoo questionnaire). The Difference between the green valley and blue cloud is distinguishable with a KS of 0.14, green valley is less distinguishable form the red sequence with a KS value of 0.06, and the KS of blue cloud and red sequence is 0.20. The significance between the green valley and blue cloud are 3.12×10^{-06} , green valley to red sequence 0.1, and blue cloud to red sequence 7.81×10^{-13} .

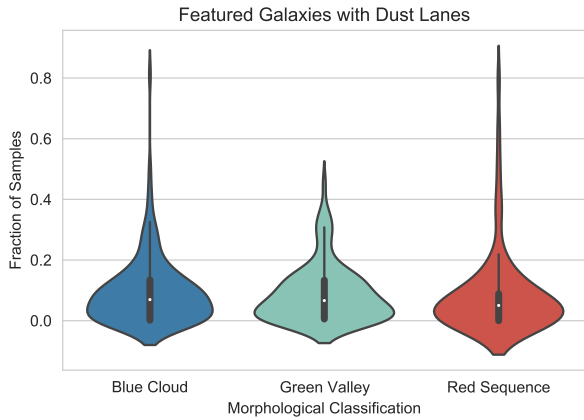
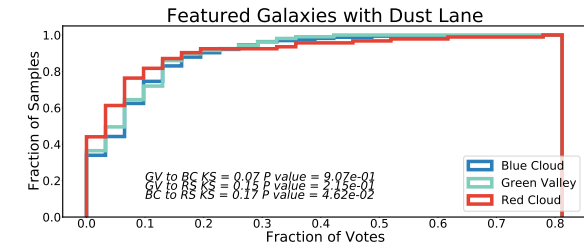


Figure A5. Histogram of the fraction of votes in favor of the galaxies having Dust Lanes (T06 in the Galaxy Zoo questionnaire). The green valley is distinguishable from the blue cloud and red sequence with a KS value of 0.08 for both, while red sequence and blue cloud are distinguishable with a KS value of 0.13. The significance between the green valley and blue cloud are 0.02 , green valley to red sequence is 0.02 , and blue cloud to red sequence is 5.36×10^{-06} .

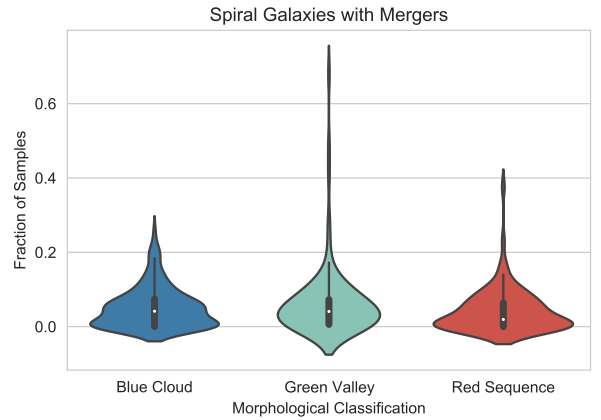
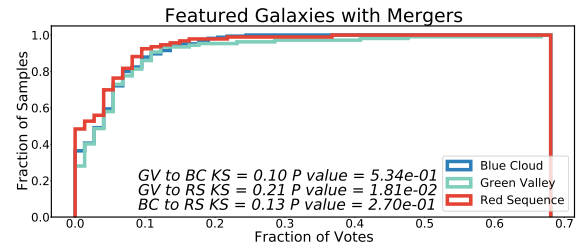


Figure A6. Histogram of the fraction of votes in favor of the galaxies having Mergers (T05 in the Galaxy Zoo questionnaire). The green valley is distinguishable from the blue cloud with a KS value of 0.09, green valley continues to be differentiated from the red sequence with a KS value of 0.12 while the red sequence and blue cloud have a KS Value of 0.18. The significance between the green valley and blue cloud are 8.05×10^{-03} , green valley to red sequence 6.8×10^{-05} , and blue cloud to red sequence 3.78×10^{-11} .

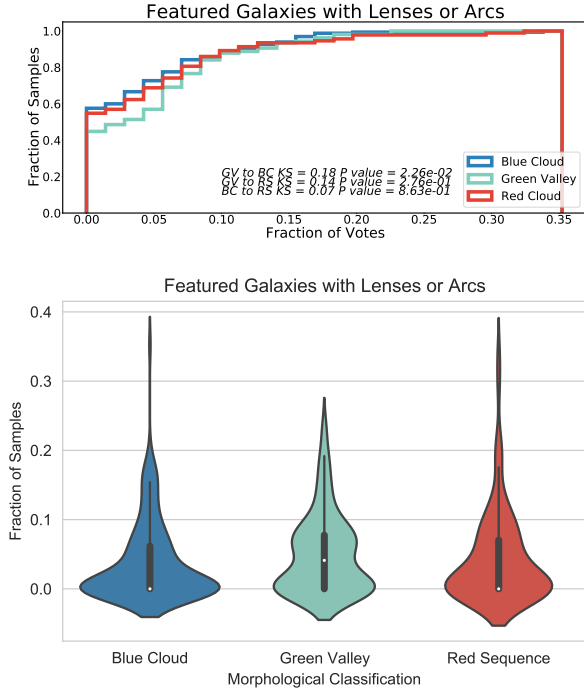


Figure A7. Histogram of the fraction of votes in favor of the galaxies having Lenses or Arcs (T06 in the Galaxy Zoo questionnaire). The green valley to blue cloud KS value is 0.04, green valley to red sequence is 0.10, and the red sequence to blue cloud has a KS Value of 0.09. The significance between the green valley and blue cloud are 0.4, green valley to red sequence 1.81×10^{-03} , and blue cloud to red sequence 6.74×10^{-03} .

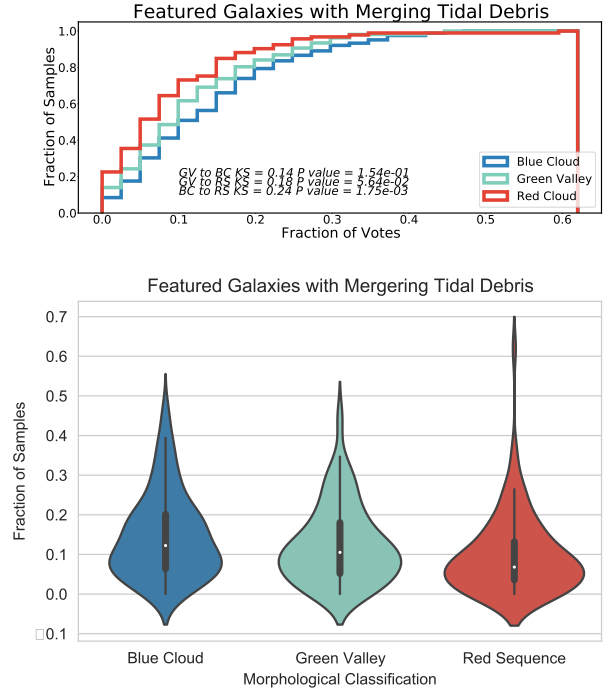


Figure A8. Histogram of the fraction of votes in favor of the galaxies having Tidal Debris (T05 in the Galaxy Zoo questionnaire). The green valley is distinguishable from the blue cloud with a KS value of 0.19, green valley continues to be differentiate from the red sequence with a KS value of 0.19 while the red sequence and blue cloud have a KS Value of 0.35. The significance between the green valley and blue cloud are 1.78×10^{-11} , green valley to red sequence 5.63×10^{-12} , and blue cloud to red sequence 3.30×10^{-39} .

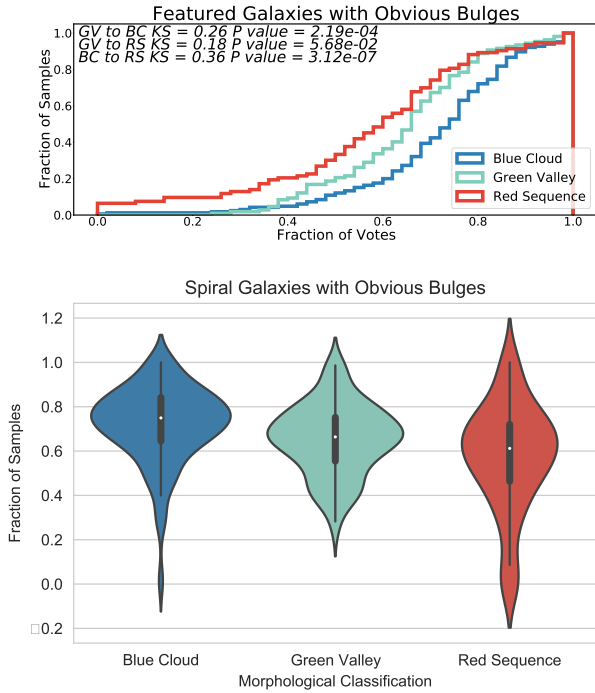


Figure A9. Histogram of the fraction of votes in favor of the galaxies having Obvious Bulges (T04 in the Galaxy Zoo questionnaire). The Difference between the green valley and blue cloud is distinguishable with a KS of 0.21, green valley is less distinguishable from the red sequence with a ks value of 0.11 staying between the behaviour of the blue cloud and red sequence which have a KS of 0.25. The significance between the green valley and blue cloud are 6.64×10^{-14} , green valley to red sequence 6.5×10^{-04} , and blue cloud to red sequence 3.66×10^{-20} .